
AppNote 7/2007

# Characterization of Organic Compounds in Atmospheric Nanoparticles by Thermal Extraction - Comprehensive Two-Dimensional Gas Chromatography (GC x GC) in Combination with Selective Detection, Mass Spectrometry and Accurate Mass Detection

Nobuo Ochiai, Teruyo Ieda, Kikuo Sasamoto
*GERSTEL K.K., 2-13-18 Nakane, Meguro-ku, Tokyo, 152-0031 Japan*

Akihiro Fushimi, Shuichi Hasegawa, Kiyoshi Tanabe, Shinji Kobayashi
*National Institute for Environmental Studies, 16-2 Onogawa, Tsukuba 305-8506, Japan*

## Keywords
Atmospheric nanoparticles, Characterization, Thermal extraction (TE), Comprehensive two-dimensional gas chromatography (GC x GC), High resolution time-of-flight mass spectrometry (HRTOF-MS), simultaneous selective and mass spectrometric detection.

## Abstract
A method for characterization of airborne particles including the nanoparticles fraction with a diameter of 29-58 nm in roadside atmosphere has been described. The method consists of thermal extraction (TE) and comprehensive two-dimensional gas chromatography (GC x GC) with novel detection capabilities, including high resolution time-of-flight mass spectrometry (HRTOF-MS), and simultaneous selective and mass spectrometric detection with a nitrogen phosphorous detector (NPD) and a quadrupole mass spectrometer (qMS). Increased selectivity with the GC x GC - HRTOF-MS allows a group type separation of a selected chemical class, e.g. oxygenated polycyclic

aromatic hydrocarbons (oxy-PAHs), using mass chromatography with a 0.05 Da wide window in the complex sample matrix. Also, accurate mass detection provides candidate elemental compositions as well as NIST library search results for tentative identifications of 50 compounds. Moreover, the simultaneous selective and mass spectrometric detection with the NPD and the qMS elucidate the presence of 15 nitrogen containing compounds. Quantitative analysis of selected PAHs in several size-resolved particles was also performed by use of the TE - GC x GC - qMS with limited scan range. The method showed good linearity ($r^2 > 0.988$) and high sensitivity (limit of quantification: < 10 pg) for most of the target PAHs.

## INTRODUCTION

Airborne particles less than 10 μm in diameter (PM10) are known to cause respiratory problems. Recently, smaller particles, e.g. nanoparticles (Diameter of particle: Dp < 50 nm) and ultrafine particles (Dp < 100 nm), have received special attention due to their potential affect to human health [1-3]. It is important to understand their toxicity, source, generation mechanism, and environmental fate. Fushimi et al indicated that organic carbon (OC) is a key chemical fraction of nanoparticles [4]. Their organic chemical compositions are, however, not fully characterized because of the small amount of sample collected (μg level) and its complexity [4, 5].

Thermal extraction (TE) - gas chromatography - mass spectrometry (TE - GC - MS) is emerging as an extraction method for organic compounds from atmospheric particles [5]. Although special attention should be paid to the possibility of pyrolysis of thermo labile compounds (e.g. long-chained alkanes and n-monocarboxylic acids) and to the matrix interference, the TE method has many practical advantages, e.g. no off-line sample preparation, small sample amount, high sensitivity, and high precision, in comparison with the traditional solvent extraction procedure. Falkovich and Rudich reported the determination of different classes of compounds such as quinoline, methylquinoline isomers, polycyclic aromatic hydrocarbons (PAHs), and n-monocarboxylic acids in the atmospheric aerosols with the TE - GC - MS [6]. Also, Hays and Smith reported the analysis of PAHs in size-resolved particles from wood combustion with the TE - GC - MS [7]. The TE - GC - MS method, however, could not provide a sufficient resolution for a separation of large numbers of organic compounds in unresolved complex mixtures (UCM) [8].

Over the past few years, comprehensive two-dimensional gas chromatography (GC x GC) [9-13] proved its large separation power in many fields of interest including air pollution research [14-16]. Also, coupling of GC x GC to a fast acquisition mass spectrometer, e.g. time-of-flight mass spectrometer (TOF-MS) with a unit-mass resolution (high speed (HS) TOF-MS), provided an improved analytical resolution of the GC x GC with mass spectral information [17, 18]. The combination of TE, GC x GC and HSTOF-MS allowed detection of more than 10,000 individual organic compounds in aerosol samples [18]. Welthagen et al proposed a search criteria and rules based on retention times and the fragmentation patterns of the GC x GC - HSTOF-MS for classification of more than 15,000 peaks in fine particulate matter (Dp < 2.5 μm) [17]. It is, however, still difficult to identify many compounds even with the structural nature and the mass spectral information provided by the GC x GC - HSTOF-MS. Hamilton et al indicated that large numbers of low-concentration compounds could not be positively identified because interpretation of mass spectral data is inconclusive with regard to structure, with many producing similar fragmentation patterns [19]. Consequently, novel, more powerful detection capabilities for GC x GC are required to given increased selectivity for identification and speciation.

In GC x GC, typical peak widths at the end of the second column can be 100-600 ms [9, 20]. Such peaks require detectors with a small internal volume, a short rise time, and a high data acquisition rate to ensure proper reconstruction of the second-dimension chromatograms. An ideal data acquisition rate should be more than 100 Hz [21]. At present, only the HSTOF-MS, e.g. Leco Pegasus (Leco, St Joseph, MI, USA), can acquire the 100 or more mass spectra per second recommended for ideal GC x GC. Recently, several authors reported the applicability of a quadrupole MS (qMS) with a rapid-scanning (10,000 Da/s) as the next best candidate MS for GC x GC compared to the HSTOF-MS. Mondello [22] et al and Ryan et al [23] reported a successful approach using a rapid-scanning qMS with a mass range of m/z 40-400 and a 20 Hz scanning rate, for qualitative analysis of perfumes and roasted coffee beans, respectively. Under these conditions, there are, however, only 3-5 data points across the fastest second-dimension peaks, which seriously compromise quantification. For proper quantification, a more limited mass range should be selected. Adahchour et al indicated that a

sufficient number of data points per peak (7-8 points) for quantification could be obtained with a mass range of m/z 50-245 and a 33 Hz scanning rate [24].

More recently, accurate mass detection (mass measurement with uncertainties of a few mDa) with fast acquisition (up to 25 Hz) have become available through recent progress in the GC-TOF-MS area. In 2005, the coupling of GC x GC to a high resolution (HR) TOF-MS with an acquisition speed of 25 Hz was reported. Ledford indicated that the acquisition speed of 25 Hz produced GC x GC contour plots of nearly the same quality as higher speed detection systems [25]. Thus, the HRTOF-MS can be considered a candidate MS which provide high-resolution mass information for qualitative analysis in GC x GC.

Simultaneous selective and MS detection is an effective method, which allows a greatly improved identification capability. Amirav et al developed a method for analysis of phosphorous pesticides by use of simultaneous pulsed flame photometric detection (PFPD) and qMS detection (1D GC - PFPD/qMS) [26]. The PFPD chromatogram could pinpoint the elution time of a suspected pesticide for a fast MS identification because of its high selectivity and retention time match with the MS. This method can be generalized as simultaneous selective and MS detection which can be extended to any other GC selective detector. Consequently, selective detectors with fast response times, e.g. micro electron capture detector (μECD), sulfur chemiluminescence detector (SCD), and nitrogen phosphorus detector (NPD), can be applied to simultaneous detection in GC x GC.

The aim of this study was to describe a new and more effective method of TE - GC x GC with the exact mass measurement using the HRTOF-MS and the simultaneous selective and MS detection using the NPD and the qMS, for characterization of atmospheric nanoparticles. Quantitative analysis of selected PAHs in several size-resolved particles was also performed by use of TE - GC x GC - qMS with a limited scan range.

## Experimental

*Material.* U. S. EPA 610 PAHs mixture containing 16 analytes was purchased from Supelco (Bellefonte, PA, USA). NAGINATA internal standard mixture containing a 5 deuterated PAH mixture was purchased from Kanto Kagaku (Tokyo, Japan). All solvents used were high-purity pesticides grade (Kanto Kagaku).

*Instrumentation.* Sampling of size-resolved particles was performed with a low-pressure impactor (LPI; DEKATI, Tampere, Finland). Analyses were performed with a GERSTEL TDS 2 thermal-desorption system equipped with a GERSTEL CIS 4 programmed temperature vaporization (PTV) inlet (Gerstel, Mülheim an der Ruhr, Germany), and a Zoex KT2004 loop type modulator (Zoex corporation, Houston, TX, USA) installed on an Agilent 6890N gas chromatograph (Agilent Technologies, Palo Alto, CA, USA) with a Micromass GCT time-of-flight mass spectrometer (Micromass, Manchester, UK) or Agilent NPD and 5973 inert MSD with high performance electronics (Agilent Technologies). Chemstation software (Agilent Technologies) and MassLynx software (Micromass) were used for raw data analysis. GC Image software (Zoex) was used for the data analysis in contour plots (2D chromatogram).

*Sampling.* Sampling was performed at the Ikegami-Shincho crossing in Kawasaki, Japan. A roadside air-pollution monitoring station is located near the crossing, where one of the worst atmospheric pollution levels in Japan was observed. The main street named “Industrial Road” has heavy traffic, especially diesel engine vehicles. Over the Industrial Road is an elevated road (Metropolitan Expressway). The northwest of the Industrial Road is a residential area, whereas the southeastern is an industrial area. The section that includes the measuring site is mainly occupied by a park and a baseball field. Buildings along the Industrial Road are generally two-stored. A vertical wall sits at the center of the Industrial Road and is about 100 m from the crossing toward Yokohama. The wall tends to make the air flow stagnant and to interfere with the wind perpendicular to the Industrial Road at ground level.

Daytime hourly-traffic (vehicles/h; from 06:00 to 21:00) was in the range of about 500 to 1600, while nighttime hourly-traffic (from 00:00 to 06:00 and from 21:00 to 24:00) was in the range of about 300 to 500. Sixty-two percent of the vehicles were categorized as having high emissions: diesel engine vehicles, e.g. buses, trucks, and trailers. Wind direction was mainly from the north and northwest during the sampling period. Thus, the sampling site was downwind of the crossing.

Size-resolved particles were collected for 24 h (January 27-28, 2004) by use of a LPI. Ungreased aluminum foils were used as the collection substance. Particles were separated into 13 size fractions according to the following equivalent cutoff diameters (aerodynamic diameters) at 50 % efficiency at a flow rate of 30 L/min: stage 1 (S1): 0.029 μm; stage 2

(S2): 0.058 μm; stage 3 (S3): 0.102 μm; stage 4 (S4): 0.163 μm; stage 5 (S5): 0.251 μm; stage 6 (S6): 0.389 μm; stage 7 (S7): 0.632 μm; stage 8 (S8): 0.980 μm; stage 9 (S9): 1.60 μm; stage 10 (S10): 2.44 μm; stage 11 (S11): 3.95 μm; stage 12 (S12): 6.54 μm; stage 13 (S13): >10.12 μm. The total suspended particles (TSP) concentration obtained from the particulate matter (PM) masses of all the impactor stage was 40.7 μg/ $m^3$. Samples were stored at -70 °C until analysis, and were divided into approximately 2.7-36 μg-PM for analyses.

*Thermal extraction.* A sample was placed in a glass thermal desorption liner with glass frit, one micro-liter of the internal standard solution (100 ng/mL) was added for quantification. Thermal extraction of a sample was performed by programming a TDS2 from 50 ºC (held for 1 min) to 350 ºC (held for 3 min) at 60 ºC/min with 50 mL/min desorption flow. Extracted compounds were cryo-focused at -100 ºC on a quartz wool packed liner in the PTV for subsequent GC-MS analysis. After desorption, the PTV inlet was programmed from -100 ºC to 330 ºC (held for 10 min) at 720 ºC/min to inject trapped compounds onto the analytical column. Injection was performed in the splitless mode with a 3 minute splitless time. During the injection, the GC was held at the initial temperature of 50 ºC.

*GC x GC - HRTOF-MS, GC x GC - NPD/qMS and GC x GC - qMS.* The GC was programmed from 50 ºC (held for 3 min) to 350 ºC at 5 ºC/min. The separation was performed on the column set of a BPX-5 fused silica capillary column (30 m x 0.25 mm i.d., 0.25 μm film thickness, SGE International, Australia) as the first column and a BPX-50 fused silica capillary column (1 m x 0.10 mm i.d., 0.10 μm film thickness, SGE International) as the second column. Helium was used as a carrier gas supplied at 2.5 mL/min for a HRTOF-MS and qMS, and 1.83 mL/min for a NPD/qMS, respectively. The modulation period was 6 s. The hot gas temperature was programmed from 250 ºC to 350 ºC at 10 ºC/min (held for 53 min). The hot gas duration time was 300 ms.

A HRTOF-MS was operated at a multi-channel plate voltage of 2600 V, a pusher interval of 38 μs (resulting in 26,316 raw spectra per second), and a mass range of m/z 45-500 using electron-impact ionization (EI; electron-accelerating voltage: 70V). The data acquisition speed was 25 Hz. A column background ion was used for single lock mass calibration with m/z 207.0329 as reference mass.

For the simultaneous detection with the NPD/qMS, the end of the second column was connected into a GERSTEL Cross-piece (Gerstel) column output splitter. The splitter output was connected to a NPD with a 45-cm long deactivated fused silica capillary column (SGE 0.10 mm I.D.) and to a qMS with a 80 cm long deactivated fused silica capillary column (SGE 0.10 mm I.D.). The pressure at the column splitter was calculated as 50 kPa with the column head pressure of 354 kPa. The flow-rate to a NPD and to a qMS was calculated to be 0.91 mL/min and 0.92 mL/min, respectively, resulting in an approximately 1:1 split ratio. NPD gas flows were 5.0 mL/min, 7.5 mL/min, and 100 mL/min for hydrogen total flow (carrier + make-up), nitrogen make-up, and air, respectively [26]. A NPD was operated at a data acquisition rate of 100 Hz. A qMS was operated in the scan mode using EI (electron-accelerating voltage: 70V). Scan range was set from m/z 54 to 280, and the acquisition speed was 18 Hz.

For a quantitative analysis of selected PAHs in size-resolved particles, a qMS with limited scan range was used. A qMS was operated in the scan mode using EI (electron-accelerating voltage: 70V). Scan range was set from m/z 177 to 280, and the acquisition speed was 27 Hz.

## Results and Discussion

*Accurate mass detection with HRTOF-MS in TE - GC x GC.* Figure 1 and 2 shows a two-dimensional (2D) total ion chromatogram (TIC) of S1 (Dp 29-58 nm; 2.7 μg-PM) obtained by the TE - GC x GC - HRTOF-MS. Although a large unresolved complex mixture (UCM) band still existed, more than a thousand peaks were separated in the 2D TIC. The signals of the UCM band and column bleeds in the lower right hand corner of the 2D TIC were completely saturated in the accurate mass detection (too intense), which resulted in serious lack of data points and mass error. These were, therefore, poor resolution in contour plots. The sensitivity of the HRTOF-MS is generally higher (e.g. down to low pg level) [28] than that of the qMS with scanning mode because of higher selectivity of exact mass and no ion loss during separation process in the flight tube (which does occur with scanning instrument such as qMS). The dynamic range of the HRTOF-MS is, however, narrower than that of the qMS because of its ion counting system, e.g. time-to-digital converter (TDC) in the GCT, and the multi-channel plate (MCP) detector. Dalluge et al indicated that the linearity of the GCT is about two or three orders of magnitude [29].

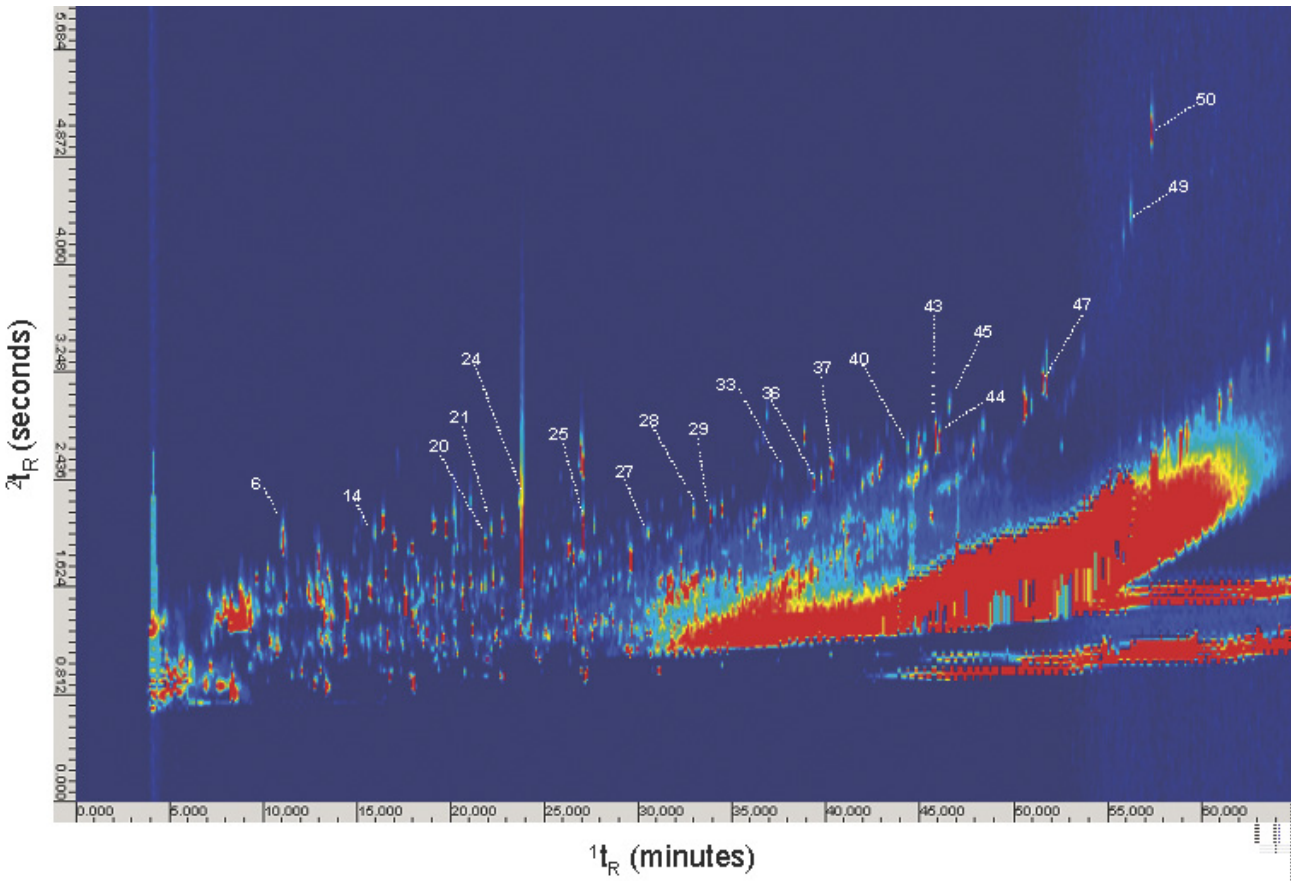


**Figure 1.** Two-dimensional total ion chromatogram obtained by TE - GC x GC - HRTOF-MS of S1 (Dp 29-58 nm; 2.7 µg-PM). The marked peaks represent tentatively identified compounds (see table 1).

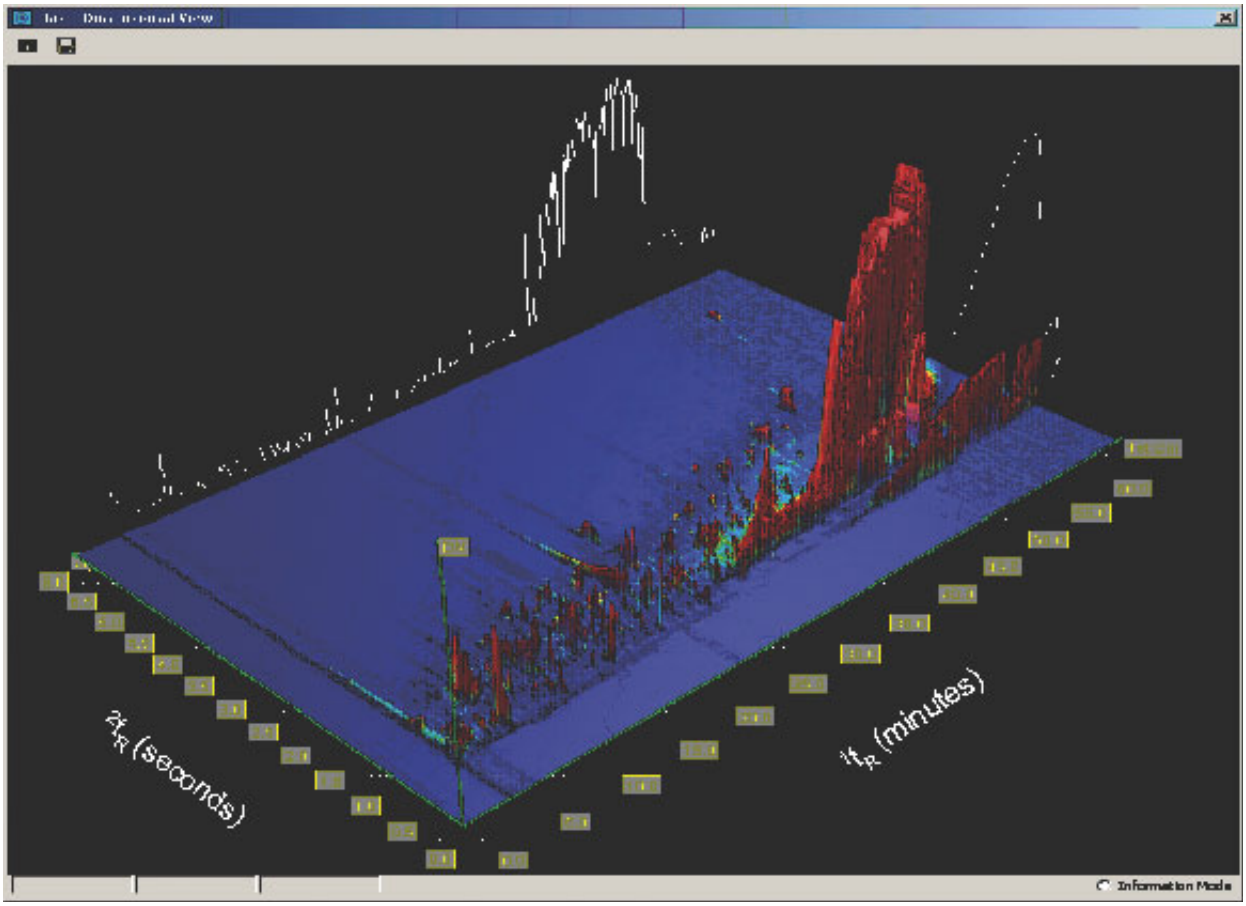


**Figure 2.** Two-dimensional total ion chromatogram obtained by TE - GC x GC - HRTOF-MS of S1 (Dp 29-58 nm; 2.7 µg-PM) in 3D landscape-plot.

As several authors indicated, there are so many different group types present in an aerosol or a PM sample [17, 18]. Using an automated NIST library search with the GC Image software, we found various chemical classes, e.g. alkanes, alkenes, cycloalkanes, long chain carboxylic acids, aldehydes, ketones, substituted aromatics, PAHs and oxy-PAHs, heterocyclic compounds and heterocyclic aromatic compounds, in the 2D chromatogram. However, most of the candidate compounds presented at trace level were still mismatched because there were large numbers of co-elution and band overlaps in the 2D TIC even with the GC x GC separation. Kallio et al [29] indicated that manual search was more accurate with the atmospheric aerosol samples, where concentrations of single compounds were rather low. In the manual identification, mass chromatography with selected ions was used for extracting analytes from the 2D TIC and it was possible to obtain high-quality spectra for good spectral match [29]. Using GC x GC - HRTOF-MS, it is possible to plot 2D mass chromatograms for individual m/z values with a 0.05 Da wide window, allowing further selectivity in the 2D mass chromatograms. This approach greatly aided not only identification but also group type separation, especially for compounds that have a unique ion such as a molecular ion in EI mass spectra. Figure 3 shows a comparison of a group type separation using the 2D mass chromatograms (sum of m/z 180.0575, 194.0732, 198.0317, 230.0732, and 258.0681) of 0.05 Da wide window and its 1.0 Da wide window for oxy-PAHs which were found earlier in urban particulate matter (e.g. PM2.5) and urban aerosols by several researchers [16, 17, 30] (e.g. m/z 180.0575: 9H-fluoren-9-one, 1H-phenalene-1-one; m/z 194.0732: 9(10H)-anthracenone; m/z 198.0317: naphtho(1,2-c)furan-1,3-dione; m/z 230.0732: 7H-benz(de)anthracen-7-one, 11H-benzo(a)fluorene-11-one; and m/z 258.0681: naphthacene-5,12-dione, benz[a]anthrace-7,12-dione).

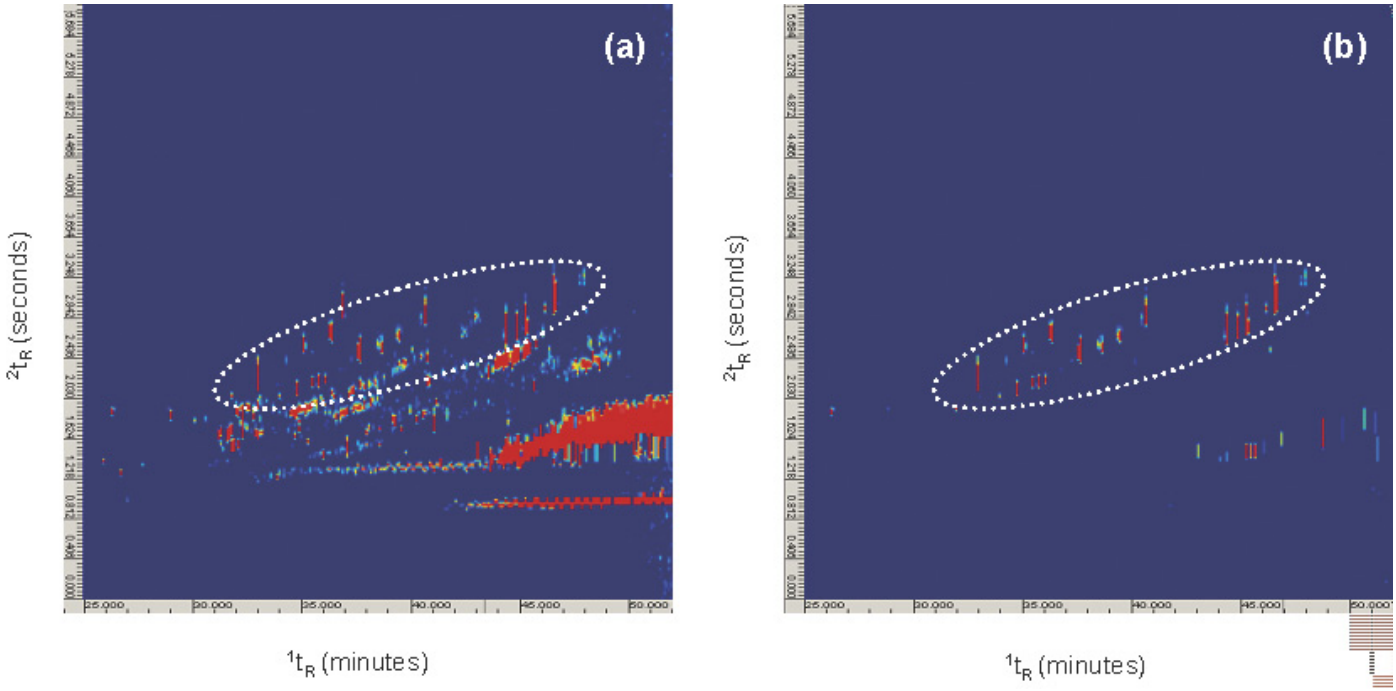


**Figure 3.** Comparison of group type separation using the two-dimensional mass chromatograms obtained by TE - GC x GC - HRTOF-MS of S1 (Dp 29-58 nm; 2.7 µg-PM) (sum of five selected ions for oxy-PAHs; m/z 180.0575, 194.0732, 198.0317, 230.0732 and 258.0681). (a) 1.0 Da wide window; (b) 0.05 Da wide window.

For the present study, tentative identification with mass chromatography with a 0.05 Da wide window, the NIST library search, and a calculation of elemental composition was manually performed for 50 compounds. The minimum reverse factor for library match and the maximum mass error for the measured m/z value were set to 800 and ±6 mDa, respectively. Elemental composition was calculated from a molecular ion. Calculation of elemental composition was performed with the average mass spectrum of all sliced peaks in the raw chromatogram. The results of tentative identification containing first column retention time ($^1t_R$), second column retention time ($^2t_R$), candidate compound name, candidate formula, reverse factor for library match, measured m/z value, theoretical m/z value, and mass error (mDa;

the difference between measured and the theoretical values) was listed in Table 1. The mass errors were in the range of - 6.0 mDa to 5.0 mDa with an average of 0.91 mDa. For 27 compounds, reasonable mass errors less than ±2 mDa with an average of 0.3 mDa were obtained. For 10 PAHs, confirmation with authentic compounds was performed.

**Table 1.** The results of tentative identification in S1 obtained by TE - GC x GC - HRTOF-MS.

| No. | $^1t_R$ [a] (min) | $^2t_R$ [b] (s) | Compounds | Formula | Reverse [c] | Measured *m/z* | Theoretical *m/z* | Mass error (mDa) |
|---|---|---|---|---|---|---|---|---|
| 1 | 7.1 | 1.02 | Toluene | $C_7H_8$ | 880 | 92.0622 | 92.0626 | -0.4 |
| 2 | 8.7 | 1.54 | Furfural | $C_5H_4O_2$ | 836 | 96.0236 | 96.0211 | 2.5 |
| 3 | 9.5 | 1.02 | Ethyl benzene | $C_8H_{10}$ | 900 | 106.0812 | 106.0783 | 2.9 |
| 4 | 10.3 | 1.17 | Styrene | $C_8H_8$ | 887 | 104.0639 | 104.0626 | 1.3 |
| 5 | 11.0 | 1.95 | 2(5H)Furanone | $C_4H_4O_2$ | 850 | 84.0225 | 84.0211 | 1.4 |
| 6 | 12.4 | 1.58 | Benzaldehyde | $C_7H_6O$ | 892 | 106.0425 | 106.0419 | 0.6 |
| 7 | 13.0 | 1.83 | 2(5H)Furanone, 3-methyl | $C_5H_6O_2$ | 924 | 98.0364 | 98.0368 | -0.4 |
| 8 | 13.1 | 1.58 | Benzonitrile | $C_7H_5N$ | 906 | 103.0362 | 103.0422 | -6.0 |
| 9 | 13.1 | 1.95 | 1H-Pyrrole-2.5-dione | $C_4H_3NO_2$ | 842 | 97.0170 | 97.0164 | 0.6 |
| 10 | 13.5 | 1.38 | Benzofuran | $C_8H_6O$ | 881 | 118.0433 | 118.0419 | 1.4 |
| 11 | 15.1 | 1.54 | Phenol, 4-methyl | $C_7H_8O$ | 864 | 108.0594 | 108.0575 | 1.9 |
| 12 | 15.7 | 1.54 | Phenol, 2-methyl | $C_7H_8O$ | 851 | 108.0570 | 108.0575 | -0.5 |
| 13 | 15.9 | 1.99 | 2,5-Furandicarboxaldehyde | $C_6H_4O_3$ | 910 | 124.0189 | 124.0160 | 2.9 |
| 14 | 16.8 | 1.50 | Benzofuran, 2-methyl | $C_9H_8O$ | 830 | 131.0536 | 131.0497 | 3.9 |
| 15 | 17.7 | 1.87 | Benzonitrile, 2-methyl | $C_8H_7N$ | 887 | 117.0613 | 117.0578 | 3.5 |
| 16 | 18.3 | 1.58 | Naphthalene | $C_{10}H_8$ | 879 | 128.0645 | 128.0626 | 1.9 |
| 17 | 20.3 | 1.91 | Benzothiazole | $C_7H_5NS$ | 842 | 135.0144 | 135.0143 | 0.1 |
| 18 | 20.7 | 1.90 | Quinoline | $C_9H_7N$ | 823 | 129.0601 | 129.0578 | 2.3 |
| 19 | 21.3 | 2.11 | Isoquinoline | $C_9H_7N$ | 877 | 129.0598 | 129.0578 | 2.0 |
| 20 | 21.8 | 1.91 | Indanone | $C_9H_8O$ | 847 | 132.0556 | 132.0575 | -1.9 |
| 21 | 22.1 | 2.03 | Indole | $C_8H_7N$ | 900 | 129.0561 | 129.0578 | -1.7 |
| 22 | 22.7 | 2.03 | Phthalic anhydride | $C_8H_4O_3$ | 898 | 148.0152 | 148.0160 | -0.8 |
| 23 | 23.5 | 1.98 | Indandione | $C_9H_6O_2$ | 875 | 146.0379 | 146.0368 | 1.1 |
| 24 | 23.8 | 1.66 | Nicotine | $C_{10}H_{14}N_2$ | 875 | 162.1161 | 162.1157 | 0.4 |
| 25 | 27.0 | 1.95 | Nicotyrine | $C_{10}H_{10}N_2$ | 838 | 158.0849 | 158.0844 | 0.5 |
| 26 | 27.9 | 1.83 | Naphtho[2,1-b]furan | $C_{12}H_8O$ | 985 | 168.0595 | 168.0575 | 2.0 |
| 27 | 30.4 | 1.99 | Benzophenone | $C_{13}H_{10}O$ | 835 | 182.0755 | 182.0732 | 2.3 |
| 28 | 32.9 | 2.15 | 9H-Fluorene-9-one | $C_{13}H_8O$ | 872 | 180.0568 | 180.0575 | -0.7 |
| 29 | 33.8 | 2.11 | Phenanthrene [d] | $C_{14}H_{10}$ | 913 | 178.0780 | 178.0783 | -0.3 |
| 30 | 34.0 | 2.19 | Anthracene [d] | $C_{14}H_{10}$ | 850 | 178.0790 | 178.0783 | 0.7 |
| 31 | 34.7 | 2.07 | Anthrone | $C_{14}H_{10}O$ | 812 | 194.0737 | 194.0732 | 0.5 |
| 32 | 36.2 | 2.68 | 1H-Phenalen-1-one | $C_{13}H_8O$ | 913 | 180.0621 | 180.0575 | 4.6 |
| 33 | 37.6 | 2.48 | 9,10-Anthracenedione | $C_{14}H_8O_2$ | 836 | 208.0545 | 208.0524 | 2.1 |
| 34 | 38.8 | 2.72 | Naphtho[1,2-c]furan-1,3-dione | $C_{12}H_6O3$ | 900 | 198.0348 | 198.0317 | 3.1 |
| 35 | 39.0 | 2.48 | Cyclopenta[def]phenanthrenone | $C_{15}H_8O$ | 879 | 204.0618 | 204.0575 | 4.3 |
| 36 | 39.3 | 2.35 | Fluoranthene [d] | $C_{16}H_{10}$ | 864 | 202.0738 | 202.0783 | -4.5 |
| 37 | 40.3 | 2.48 | Pyrene [d] | $C_{16}H_{10}$ | 886 | 202.07265 | 202.0783 | -5.7 |
| 38 | 41.9 | 2.40 | Pyrene, 2-methyl | $C_{17}H_{12}$ | 845 | 216.0989 | 216.0939 | 5.0 |
| 39 | 42.4 | 2.44 | Pyrene, 1-methyl | $C_{17}H_{12}$ | 868 | 216.0971 | 216.0939 | 3.2 |
| 40 | 44.3 | 2.68 | 11H-Benzo[a]fluoren-11-one | $C_{17}H_{10}O$ | 851 | 230.0771 | 230.0732 | 3.9 |
| 41 | 44.9 | 2.68 | Benzo[ghi]fluoranthene | $C_{18}H_{10}$ | 827 | 226.0811 | 226.0783 | 2.8 |
| 42 | 45.8 | 2.80 | Cyclopenta[cd]pyrene | $C_{18}H_{10}$ | 844 | 226.0751 | 226.0783 | -3.2 |
| 43 | 45.8 | 2.68 | Benzo[a]anthracene [d] | $C_{18}H_{12}$ | 863 | 228.0911 | 228.0939 | -2.8 |

**Table 1 (cont.).** The results of tentative identification in S1 obtained by TE - GC x GC - HRTOF-MS.

| No. | $^1t_R$ [a] (min) | $^2t_R$ [b] (s) | Compounds | Formula | Reverse [c] | Measured *m/z* | Theoretical *m/z* | Mass error (mDa) |
|---|---|---|---|---|---|---|---|---|
| 44 | 46.0 | 2.68 | Chrysene [d] | $C_{18}H_{12}$ | 836 | 228.0922 | 228.0939 | -1.7 |
| 45 | 46.5 | 2.96 | 7H-Benzo[de]anthracen-7-one | $C_{17}H_{10}O$ | 831 | 230.0748 | 230.0732 | 1.6 |
| 46 | 47.6 | 2.64 | Chrysene, 1-methyl | $C_{19}H_{14}$ | 819 | 242.1137 | 242.1096 | 4.1 |
| 47 | 51.7 | 3.13 | Benzo[a]pyrene [d] | $C_{20}H_{12}$ | 827 | 252.0921 | 252.0939 | -1.8 |
| 48 | 52.0 | 3.25 | Perylene [d] | $C_{20}H_{12}$ | 823 | 252.0951 | 252.0939 | 1.2 |
| 49 | 56.2 | 4.43 | Indeno[1,2,3-cd]pyrene [d] | $C_{22}H_{12}$ | 929 | 276.0965 | 276.0939 | 2.6 |
| 50 | 57.3 | 5.08 | Benzo[ghi]perylene [d] | $C_{22}H_{12}$ | 818 | 276.0965 | 276.0939 | 2.6 |

[a] First column retention time (min)
[b] Second column retention time (s)
[c] Reverse factor for the NIST library search
[d] Confirmation with authentic compound was performed

Continuous introduction of a calibration compound, e.g. 2,4,6-Tris-trifluoromethyl-[1,3,5]triazine, during each analysis may compensate for the mass error. However, its mass spectrum (containing m/z 68.9952, 121.0014, 189.9966, 265.9964 and 284.9949) is superimposed on all other mass spectra. Thus, these spectra have to be subtracted from the raw data prior to the data conversion to 2D contour plots. In our case, data conversion from the background-subtracted data to 2D contour plots failed with the GC Image software version 1.7. Therefore, only a single lock mass calibration with a column background ion (m/z 207.0329) was performed for the present study.

*Simultaneous selective and MS detection with the NPD/qMS in TD - GC x GC.* In GC x GC, a combination of elemental selective detection and the MS aids identification of unknown compounds containing a specific hetero-element. van Stee et al [31] reported the correlated use of GC x GC - atomic emission detector (AED) with S-selective detection and GC x GC - HSTOF-MS for identification of unknown sulfur compounds in fluidized catalytic cracking (FCC) oil. However, direct matching of GC x GC - AED and GC x GC - HSTOF-MS could not be done because retention times in both dimensions are different.

Using TE - GC x GC - HRTOF-MS, we tentatively identified several nitrogen containing compounds in S1 (Dp 29-58 nm) and S2 (Dp 58-102 nm). In order to confirm the presence of nitrogen containing compounds, we applied simultaneous detection with the NPD and the qMS to TE - GC x GC analysis of S2, which enabled direct matching of the 2D NPD chromatogram and the 2D TIC. Figure 4 shows a comparison of 2D chromatograms obtained by the TE - GC x GC - NPD/qMS. The 2D NPD chromatogram elucidates the spots for the nitrogen and phosphorus containing compounds in the complex sample matrix. Also, the 2D NPD chromatogram can serve as a marker for the elution time of those compounds in the 2D TIC. The resulting mass spectra obtained at the elution times identified by NPD were used for the NIST library search. For seven spots, the candidate nitrogen-containing compounds from the NIST library search were the same as those obtained from the accurate mass detection. Also, eight more nitrogen containing compounds were tentatively identified with the reverse factor of more than 812. These eight compounds were not identified with the TE - GC x GC - HRTOF-MS because the reverse factor and/or the mass errors were outside of the acceptance criteria (reverse factor: >800; mass error: <±6 mDa). For 15 nitrogen containing compounds, the NPD chromatogram and the 2D TIC showed same retention times in the first column separation. The time differences between the 2D NPD chromatogram and the 2D TIC in the second column separation were in the range of 0.12 s to 0.25 s with an average of 0.17 s. Table 2 shows the first column retention time ($^1t_R$), the second column retention time ($^2t_R$), candidate compound name, candidate formula, and the reverse factor for library match.

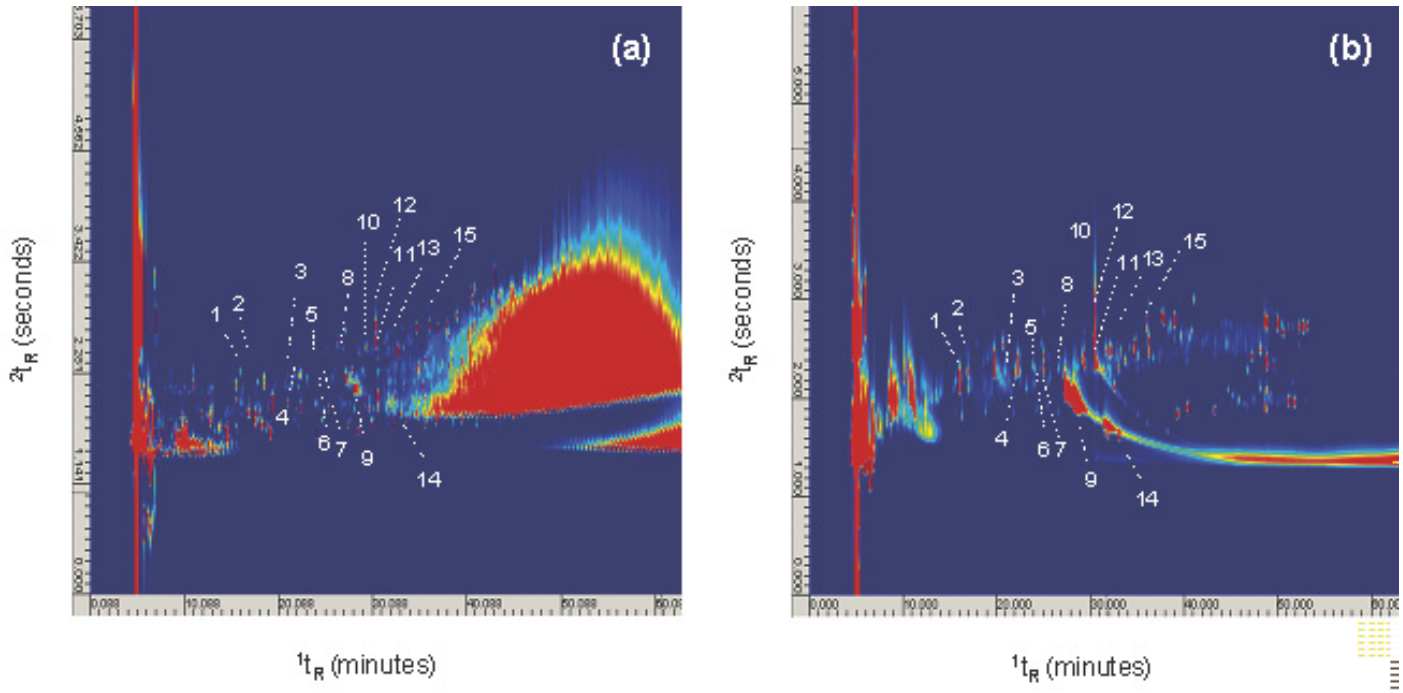


**Figure 4.** Comparison of the two-dimensional chromatograms obtained by TE - GC x GC - NPD/qMS of S2 (Dp 58-102 nm; 4.6 µg-PM). (a) total ion chromatogram; (b) NPD chromatogram. The marked peaks represent tentatively identified nitrogen-containing compounds (see table 2).

**Table 2.** The results of tentative identification for nitrogen containing compounds in S2 obtained by TE - GC x GC - NPD/qMS

| No. | $^1t_R$ [a] (min) NPD | $^2t_R$ [a] (s) NPD | $^1t_R$ [a] (min) qMS | $^2t_R$ [a] (s) qMS | Compounds | Formula | Reverse [c] |
|---|---|---|---|---|---|---|---|
| 1 | 16.0 | 2.11 | 16.0 | 2.28 | Benzonitrile | $C_7H_5N$ | 914 |
| 2 | 16.8 | 2.25 | 16.8 | 2.40 | 3-Pyridinecarbonitrile | $C_6H_4N_2$ | 877 |
| 3 | 20.9 | 2.27 | 20.9 | 2.40 | Benzonitrile, 4-methyl | $C_8H_7N$ | 898 |
| 4 | 21.9 | 2.24 | 21.9 | 2.40 | 2-chloro-benzonitrile | $C_7H_4ClN$ | 897 |
| 5 | 23.8 | 2.33 | 23.8 | 2.45 | Benzothiazole | $C_7H_5NS$ | 917 |
| 6 | 24.1 | 2.30 | 24.1 | 2.45 | Quinoline | $C_9H_7N$ | 905 |
| 7 | 24.9 | 2.28 | 24.9 | 2.45 | Isoquinoline | $C_9H_7N$ | 886 |
| 8 | 26.5 | 2.29 | 26.5 | 2.45 | 2,4-Dichlorobenzonitrile | $C_7H_3Cl_2N$ | 877 |
| 9 | 28.2 | 1.93 | 28.2 | 2.05 | Nicotine | $C_{10}H_{14}N_2$ | 920 |
| 10 | 29.2 | 2.35 | 29.2 | 2.51 | Miosmine | $C_9H_{10}N_2$ | 904 |
| 11 | 30.4 | 2.40 | 30.4 | 2.57 | Nicotyrine | $C_{10}H_{10}N_2$ | 888 |
| 12 | 30.4 | 2.72 | 30.4 | 2.97 | Phthalimide | $C_8H_5NO_2$ | 817 |
| 13 | 32.0 | 2.47 | 32.0 | 2.68 | 2,3-Bipyridine | $C_{10}H_8N_2$ | 838 |
| 14 | 33.0 | 1.61 | 33.0 | 1.83 | 2.2'-Diethyldihexylamine | $C_{16}H_{35}N$ | 812 |
| 15 | 35.9 | 2.71 | 35.9 | 2.91 | Cotinine | $C_{10}H_{12}N_2O$ | 869 |

[a] First column retention time (min)
[b] Second column retention time (s)
[c] Reverse factor for the NIST library search

*Quantitative analysis of PAHs in size-resolved particles.* To validate the TE - GC x GC - qMS method, we first evaluated linearity, limit of quantification (LOQ), and repeatability with 12 PAHs. The selected ions used for quantification and the results are shown in Table 3. Correlation coefficients ($r^2$) at five levels between 10 and 500 pg were in the range of 0.980 to 0.998. The signal-to-noise ratio obtained for the largest sliced peak in the raw chromatogram at the lowest level was used to calculate the LOQ at a signal-to-noise ratio of ten. Very low LOQ in the range of 0.79-11 pg was obtained. Repeatability was also assessed by replicate analyses (n = 5) of the middle level of the calibration curve (100 pg). The repeatability of retention times for both

first column and second column were very good with low relative standard deviation (RSD) in the range of 0.0-0.86 %. The repeatability of selected ion response was also good with RSD in the range of 2.8-8.2 %. The method was applied to several size-resolved particles such as S1 (Dp 29-58 nm; 5.6 µg-PM), S3 (Dp 102-163 nm; 36 µg-PM) and S9 (Dp 1.60-2.44 µm; 36 µg-PM). Figure 5 shows 2D mass chromatograms (sum of m/z 178, 202, 228, 252, 276, and 278) obtained by the TE - GC x GC - qMS of S1 in 3D landscape-plot. Figure 6 shows the comparison of the PAHs concentration per PM mass. For all analytes, the PM concentrations of S1 (4.2-39 pg/µg-PM) were remarkably higher than those of larger size particles such as S3 (0.44-20 pg/µg-PM) and S9 (1.6-17 pg/µg-PM). Also, the concentration per PM mass of benzo(g,h,i)pelyrene which has the lowest vapor pressure was dominant in S1.

**Table 3.** Linearity, repeatability and LOQ for selected PAHs by TE - GC x GC - qMS.

| | Abbreviation | *m/z* [a] | Linearity ($r^2$) | Repeatability [b] (RSD %, n = 5) | | | LOQ [c] (pg) |
|---|---|---|---|---|---|---|---|
| | | | | Response | $^1t_R$ (min) | $^2t_R$ (s) | |
| Phenanthrene | PHE | 178 | 0,995 | 6,7 | 0,12 | 0,86 | 0,79 |
| Anthracene | ANT | 178 | 0,994 | 6,9 | 0,00 | 0,00 | 1,2 |
| Fluoranthene | FLU | 202 | 0,998 | 2,8 | 0,13 | 0,00 | 0,58 |
| Pyrene | PYR | 202 | 0,995 | 4,6 | 0,00 | 0,00 | 0,85 |
| Benzo [a] anthracene | BAA | 228 | 0,995 | 3,7 | 0,00 | 0,75 | 4,4 |
| Chrysene | CRY | 228 | 0,997 | 3,5 | 0,11 | 0,00 | 3,7 |
| Benzo [b] fluoranthene | BBKF | 252 | Σ= 0.981 | Σ= 4.2 | Σ= 0.00 | Σ= 0.73 | Σ= 9.2 |
| Benzo [k] fluoranthene | | | | | | | |
| Benzo [a] pyrene | BAP | 252 | 0,980 | 4,9 | 0,00 | 0,00 | 5,2 |
| Indeno [1,2,3-cd] pyrene | IND | 276 | 0,988 | 8,2 | 0,00 | 0,00 | 4,6 |
| Dibenzo [a,h] anthracene | DAH | 278 | 0,988 | 6,6 | 0,00 | 0,53 | 11 |
| Benzo [g,h,i] perylene | BHG | 276 | 0,994 | 4,5 | 0,00 | 0,00 | 7,1 |

[a] Selected ions used for method validation
[b] Repeatability was assessed by replicate analyses (n = 5) of the middle level of calibration curve (100 pg)
[c] The signal-to-noise ratio obtained for the smallest sliced peak in the raw chromatogram at the lowest level was used to calculate the LOQ at a signal-to-noise ratio of ten

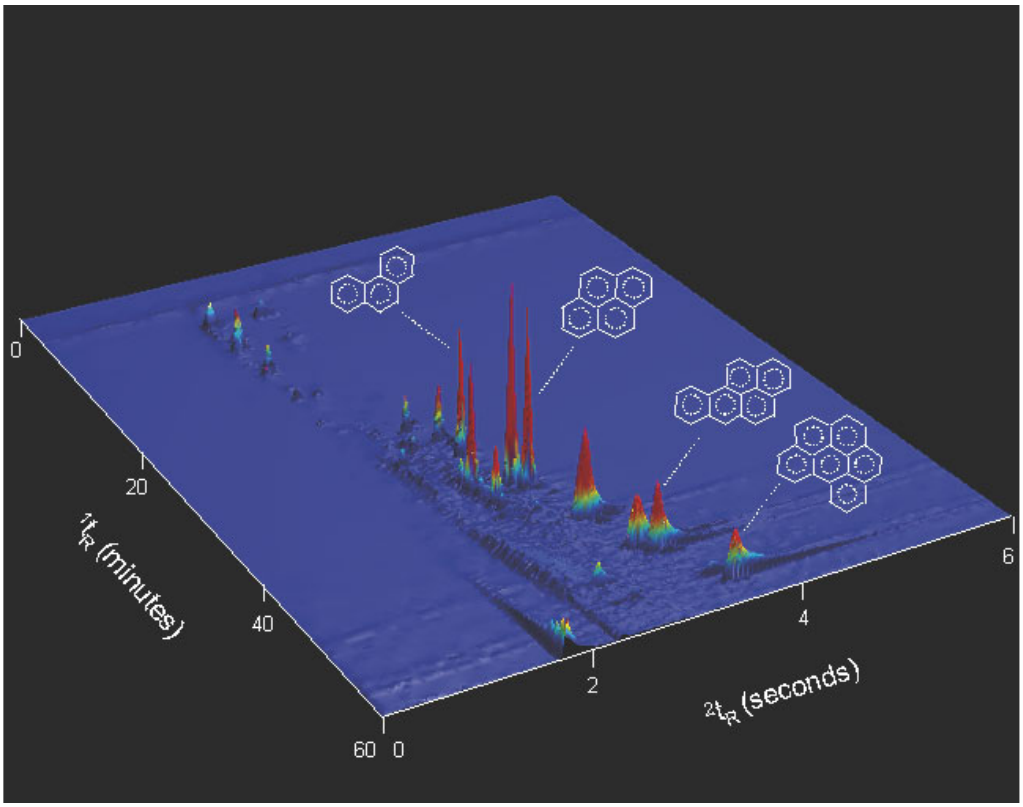


**Figure 5.** Two-dimensional mass chromatograms obtained by TE - GC x GC - qMS of S1 (Dp 29-58 nm; 5.6 µg-PM) in 3D landscape-plot (sum of six selected ions for PAHs; m/z 178, 202, 228, 252, 276 and 278).

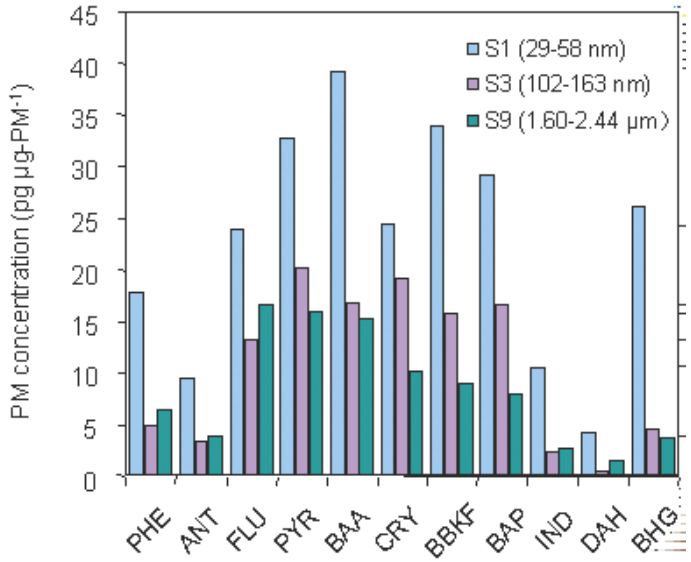


**Figure 6.** Comparison of the concentration per PM mass of selected PAHs in size-resolved particles.

## Conclusion

A combined method consisting of thermal extraction, GC x GC, HRTOF-MS, NPD and qMS for characterization of nanoparticles in roadside atmosphere was described. Fifty compounds were tentatively identified in the nanoparticle fraction (Dp: 29-58 nm) by TE - GC x GC - HRTOF-MS utilizing manual identification procedures, e.g. mass chromatography with a 0.05 Da wide window, the NIST library search, and calculation of elemental composition. Also, simultaneous selective and MS detection with the NPD and the qMS in TE - GC x GC allowed a direct matching of the 2D NPD chromatogram and the 2D TIC for tentative identification of 15 nitrogen containing compounds. Moreover, by using TE - GC x GC - qMS with limited scan range and acquisition speed of 27 Hz, ultra-trace level (pg/µg-PM) of selected PAHs in size resolved particles could be determined.

## Acknowledgements

The authors thank Mr. Toshifumi Miyawaki of Jasco International Co., Ltd., our colleagues Mr. Edward A. Pfannkoch of GERSTEL Inc. and Mr. Hirooki Kanda of GERSTEL K.K for their kind support and technical comment. Jasco International Co., Ltd. is also thanked for the use of the Micromass GCT.

## References

[1] G. Oberdorster, Int. Arch. Occup. Environ. Health, 74 (2001) 1.
[2] D. M. Brown, M. R. Wilson, W. MacNee, V. Stone, K. Donaldson, Toxicol. Appl. Pharm., 175 (2001) 191.
[3] K. Inoue, H. Takano, R. Yanagisawa, M. Sakurai, T. Ichinose, K. Sadakane, T. Yoshikawa, Respiratory Research, 6 (2005) 106.
[4] A. Fushimi, S. Hasegawa, Y. Fujitani, K. Tanabe, S. Kobayashi, in: Abstracts of European Aerosol Conference 2005, Ghent, Belgium, 28 August-2 September 2005, European Aerosol Assembly, p.633.
[5] M. D. Hays, R. J. Lavrich, Trends Anal. Chem., 26 (2006) 88.
[6] A. H. Falkovich, Y. Rudich, Environ. Sci. Technol., 35 (2001) 2326.
[7] M. D. Hays, N. D. Smith, J. Kinsey, Y. Dong, P. Kariher, Aerosol Science, 34 (2003) 1061.
[8] M. D. Hays, N. D. Smith, Y. Dong, J. Geophys. Res., 109 (2004) D16S04.
[9] J. Phillips, J. Beens, J. Chromatogr. A, 856 (1999) 331.
[10] P. J. Marriott, R. Shellie, Trends Anal. Chem., 21 (2002) 573.
[11] J. D. Dimandja, Anal. Chem. 76 (2004) 167A.
[12] T. Gorecki, J. Harynuk, O. Panic, J. Sep. Sci., 27 (2004) 359.
[13] J. Beens, U. A. Th. Brinkman, Analyst 130 (2005) 123.
[14] A. C. Lewis, N. Carslaw, P. J. Marriott, R. M. Kinghorn, P. Morrison, A. L. Lee, K. D. Bartle, M. J. Pilling, Nature 405 (2000) 778.
[15] J. F. Hamilton, A. C. Lewis, Atomos. Envir., 37 (2003) 589.
[16] M. Kallio, T. Hyotylainen, M. Lehtonen, M. Jussila, K. Hartonen, M. Shimmo, M-L. Riekkola, J. Chromatogr. A, 1019 (2003) 251.
[17] W. Welthagen, J. Schnelle-Kreis, R. Zimmermann, J. Chromatogr. A, 1019 (2003) 233.
[18] J. F. Hamilton, P. J. Webb, A. C. Lewis, J. R. Hopkins, S. Smith, P. Davy, Atmos. Chem. Phys., 4 (2004) 1279.
[19] J. F. Hamilton, P. J. Webb, A. C. Lewis, M. M. Reviejo, Atmos. Envir., 39 (2005) 7263.
[20] J. Dalluge, J. Been, U. A. Th. Brinkman, J. Chromatogr. A, 1000 (2003) 69.
[21] M. Adahchour, J. Been, R. J. J. Vreuls, U. A. Th. Brinkman, Trends Anal. Chem., 25 (2006) 540.

[22] L. Mondello, A. Casilli, P. Q. Tranchida, G. Dugo, P. Dugo, J. Chromatogr. A, 1067 (2005) 235.
[23] D. Ryan, R. Shellie, P. Q. Tranchida, A. Casilli, L. Mondello, P. Marriott, J. Chromatogr. A, 1054 (2004) 57.
[24] M. Adahchour, M. Brandt, H. -U. Baier, R. J. J. Vreuls, A. M. Batenburg, U. A. Th. Brinkman, J. Chromatogr. A, 1054 (2004) 57.
[25] E. Ledford, in: Abstracts of 28th ISCC, Las Vegas, Nevada, USA, 2005, CD-ROM 0272.
[26] A. Amirav, H. Jing, J. Chromatogr. A, 814 (1998) 133.
[27] D. Ryan, P. Watkins, J. Smith, M. Allen, P. Marriott, J. Sep. Sci., 28 (2005) 1075.
[28] J. Dalluge, P. Roose, U. A. Th. Brinkman, J. Chromatogr. A, 970 (2002) 213.
[29] M. Kallio, M. Jussila, T. Rissanen, P. Anttila, K. Hartonen, A. Reissell, R. Vreuls, M. Adahchour, T. Hyotylainen, J. Chromatogr. A, 1125 (2006) 234.
[30] J. Schnelle-Kreis, M. Sklorz, A. Peters, J. Cyrys, R. Zimmermann, Atmos. Envir., 39 (2005) 7702.
[31] L. L. P. van Stee, J. Been, R. J. J. Vreuls, U. A. Th. Brinkman, J. Chromatogr. A, 1019 (2003) 89.

G L O B A L  A N A L Y T I C A L  S O L U T I O N S


**GERSTEL GmbH & Co. KG**
Eberhard-Gerstel-Platz 1
45473 Mülheim an der Ruhr
Germany
☎ +49 (0) 208 - 7 65 03-0
🖷 +49 (0) 208 - 7 65 03 33
@ gerstel@gerstel.com
🌐 www.gerstel.com

## GERSTEL Worldwide

**GERSTEL, Inc.**
701 Digital Drive, Suite J
Linthicum, MD 21090
USA
☎ +1 (410) 247 5885
🖷 +1 (410) 247 5887
@ sales@gerstelus.com
🌐 www.gerstelus.com

**GERSTEL AG**
Wassergrabe 27
CH-6210 Sursee
Switzerland
☎ +41 (41) 9 21 97 23
🖷 +41 (41) 9 21 97 25
@ swiss@ch.gerstel.com
🌐 www.gerstel.ch

**GERSTEL K.K.**
1-3-1 Nakane, Meguro-ku
Tokyo 152-0031
SMBC Toritsudai Ekimae Bldg 4F
Japan
☎ +81 3 5731 5321
🖷 +81 3 5731 5322
@ info@gerstel.co.jp
🌐 www.gerstel.co.jp

**GERSTEL LLP**
Level 25, North Tower
One Raffles Quay
Singapore 048583
☎ +65 6622 5486
🖷 +65 6622 5999
@ SEA@gerstel.com
🌐 www.gerstel.com

**GERSTEL Brasil**
Av. Pascoal da Rocha Falcão, 367
04785-000 São Paulo - SP Brasil
☎ +55 (11)5665-8931
🖷 +55 (11)5666-9084
@ gerstel-brasil@gerstel.com
🌐 www.gerstel.com.br



Awarded for the
active pursuit of
environmental sustainability